

LAMINAR FILM CONDENSATION
IN ZERO GRAVITY

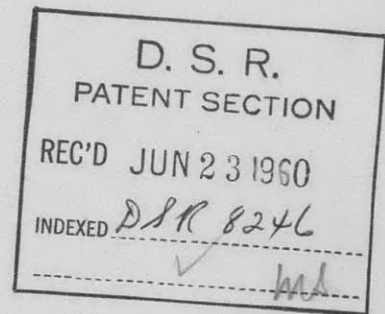
by

A. H. Stenning

R. J. Hooper

D. H. Korn

Y. Yoshitani



Nuclear Engineering Department
Massachusetts Institute of Technology
Cambridge, Mass. June 1960

Final report on contract DSR 8246, performed for the
Pratt and Whitney Aircraft Division of the United
Aircraft Corporation

Laminar Film Condensation
in Zero Gravity

by

A. H. Stenning*

R. J. Hooper†

D. H. Korn†

Y. Yoshitani†

Abstract

An approximate theory of laminar film condensation has been developed for a vapor condensing on a plate under the action of shear forces with no gravitational force. Experiments on vapor condensation in a horizontal duct suggest that the theory may be used for the design of condensers in zero gravity.

* Assistant Professor of Nuclear Engineering
MIT Cambridge, Mass.

† Research Assistant, Department of Nuclear Engineering
MIT Cambridge, Mass.

Acknowledgements

The work described below was carried out at MIT under the sponsorship and with the financial support of the Pratt and Whitney Division of the United Aircraft Corporation. The valuable suggestions of Mr. P. Bolan are gratefully acknowledged.

1. INTRODUCTION

Boundary layer theory was first applied to the film condensation of a vapor on a cold vertical or inclined plate by Nusselt in 1916 (Ref. 1). As is shown in Figure 1, the liquid condenses on the surface, and runs down it under the influence of gravitational force. Equilibrium between the body forces and the shear force exerted by the plate on the liquid produces a thin laminar film whose thickness is proportional to the square root of the distance x from the leading edge of the plate. When the film Reynolds Number exceeds 1200, transition from laminar to turbulent flow may occur in the film.

Nusselt's analysis neglected momentum effects in the film, liquid subcooling, and vapor shear stress. Later workers (Ref. 2, 3, 4) included some or all of these effects, obtaining corrections to Nusselt's basic equation which is, however, still adequate for design purposes in most cases.

In the absence of gravity forces (or under conditions of free fall) the liquid condensing on the plate will not run off unless the vapor is in

motion over the film so that the shear stress exerted by the vapor on the film drags the condensate away. If the vapor is flowing through a duct and condensing on the walls there will be pressure forces acting on the film in addition to the variable shear forces.

In section 2, boundary layer integral methods are used to predict the film growth and heat transfer coefficients for several configurations.

2. ANALYSIS

2.1 Equations

Consider the laminar film condensation of a saturated vapor flowing over a cold, flat surface. A portion of the film is shown in Figure 2.

The vapor exerts a shear stress τ_v on the surface of the film. The wall exerts a shear stress τ_w on the other boundary of the film.

In the steady state, we can write the following differential equations for the condensate layer (see glossary for definitions of symbols).

$$\text{Momentum} \quad u \frac{\partial u}{\partial x} + v \frac{\partial u}{\partial y} + \frac{g_0}{\rho} \frac{\partial p}{\partial x} = \nu \frac{\partial^2 u}{\partial y^2} \quad (1)$$

$$\text{Continuity} \quad \frac{\partial u}{\partial x} + \frac{\partial v}{\partial y} = 0 \quad (2)$$

$$\text{Energy} \quad u \frac{\partial T}{\partial x} + v \frac{\partial T}{\partial y} = \frac{K}{\rho C} \frac{\partial^2 T}{\partial y^2} \quad (3)$$

It is convenient to rewrite these equations in integral form, so that assumed velocity and temperature distributions may be substituted directly

(6)

to give approximate solutions. The integral equations are

$$\text{Momentum} \quad g_0(\tau_v - \tau_w) - \frac{dp}{dx} \cdot \delta \cdot g_0 = \frac{d}{dx} \left[\int_0^\delta \rho u^2 dy \right] - u_\delta \frac{d}{dx} \left[\int_0^\delta \rho u dy \right]$$

(4)

$$\text{Energy} \quad K \left(\frac{\partial T}{\partial y} \right)_{y=0} = \frac{d}{dx} \left[\int_0^\delta \rho u \left[\lambda + C(T_s - T) \right] dy \right]$$

(5)

with boundary conditions

$$\underline{y = 0} \quad u=0 \quad \frac{\mu}{g_0} \left(\frac{\partial u}{\partial y} \right) = \tau_w$$

$$\frac{\mu}{g_0} \left(\frac{\partial^2 u}{\partial y^2} \right) = \frac{dp}{dx} \frac{\mu}{g_0} \left(\frac{\partial^3 u}{\partial y^3} \right) = 0$$

$$\underline{y = \delta} \quad \frac{\mu}{g_0} \left(\frac{\partial u}{\partial y} \right) = \tau_v \quad K \frac{\partial T}{\partial y} = \frac{d}{dx} \left[\int_0^\delta \rho u \lambda dy \right]$$

$$u = u_\delta$$

These equations may now be applied to solve situations of increasing complexity. They are also valid for curved surfaces if $\delta \ll R$ where R is the radius of curvature.

2.2 Flat plate with zero pressure gradient and constant film ΔT

Saturated vapor flows over a long flat plate until an essentially x -independent fully developed shear flow has formed, with the vapor exerting a shear stress τ_v on the wall. At $x=0$, the surface temperature of the plate is lowered to a value ΔT below the saturation temperature of the fluid and is kept constant at this value for $x > 0$. The vapor condenses on the plate, forming a film. The vapor velocity remains constant and so does the vapor shear stress τ_v , since the film velocity is so small that the boundary condition on the vapor is essentially unchanged.

If $C\Delta T \ll \lambda$, the difference between the heat flux normal to the film at $y=\delta$ and $y=0$ can be neglected. Then $\frac{\partial T}{\partial y}$ is constant throughout the film, and equal to $\frac{\Delta T}{\delta}$. This approximation will be used throughout the analysis. The error which it introduces is negligible if $C\Delta T < 0.15\lambda$. Using a cubic equation to represent the film y -velocity distribution, we find that the boundary conditions are satisfied by the following equation

$$u = \frac{g_0}{3\mu}(\tau_v - \tau_w) \frac{y^3}{\delta^2} + \frac{\tau_w g_0}{\mu} y \quad (6)$$

(8)

The momentum equation becomes

$$60g_0(\tau_v - \tau_w) \frac{\mu^2}{\rho} = \frac{\delta^2}{21}(194\tau_w - 47\tau_v) \frac{d\tau_w}{dx} + \frac{\delta^2}{21}(116\tau_w^2 - 106\tau_w\tau_v - 10\tau_v^2) \frac{d\delta}{dx} \quad (7)$$

The energy equation may be written

$$\frac{6K\Delta T\mu}{g_0\rho} = \delta^2 \left[\tau_w \left(5\lambda + \frac{9}{5} C\Delta T \right) + \tau_v \left(\lambda + \frac{C\Delta T}{5} \right) \right] \frac{d\delta}{dx} + \delta^3 \left[\frac{5}{2} \lambda + \frac{9}{10} C\Delta T \right] \frac{d\tau_w}{dx} \quad (8)$$

These equations have the simple solution

$$\tau_w = \text{constant}$$

$$\delta^{3/x} = \text{constant}$$

Moreover, τ_w is only one or two percent smaller than τ_v for all cases of practical interest. In consequence,

(9)

the momentum equation can be neglected and τ_w taken as equal to τ_v without significant error. Thus equation (6) reduces to

$$u = \frac{\tau_v g_0}{\mu} y \quad (9)$$

The momentum equation contracts to $\tau_w = \tau_v$, and the energy equation becomes

$$\frac{2\mu K \Delta T}{g_0 \rho (\lambda + C \frac{\Delta T}{3})} = \delta \frac{d}{dx} (\tau_v \delta^2) \quad (10)$$

with the solution

$$\delta = \left[\frac{3K \Delta T \mu x}{\rho g_0 \tau_v \lambda'} \right]^{1/3} \quad (11)$$

where $\lambda' = \lambda + \frac{C \Delta T}{3}$

Over a distance x , the heat removed is equal to the quantity of fluid condensed multiplied by λ' . Equating the heat transferred to $h_m \Delta T x$ where h_m is the average film heat transfer coefficient we find

$$h_m \Delta T x = \frac{\rho g_0 \tau_v}{2\mu} \delta^2 \lambda' \quad (12)$$

(10)

whence

$$h_m = 1.04K \left[\frac{\rho \tau_v g_o \lambda'}{K \Delta T \mu x} \right]^{1/3} \quad (13)$$

In dimensionless form $\frac{h_m x}{K} = 1.04 \left[\frac{\rho \tau_v g_o \lambda' x^2}{K \Delta T \mu} \right]^{1/3} \quad (14)$

For practical values of vapor shear stress, the heat transfer coefficients are found to be an order of magnitude smaller than those for normal earth-gravity condensation on vertical plates. The Nusselt number predicted by equation (14) is plotted in Figure 3.

2.3 Condensation in Flow between two flat plates.

Constant film ΔT .

Consider a flowing vapor condensing on one or both surfaces of a duct formed by two parallel flat plates of spacing a (Figure 4). With condensation occurring in an enclosed space, the vapor volume will decrease by an amount proportional to the fraction of the vapor condensed. At the same time, the increasing thickness of the vapor film will reduce the flow area for the remaining vapor. This investigation is concerned only with that portion of the process for

(11)

which the film is laminar. In this region, the film thickness is generally so small with respect to the plate spacing that an order of magnitude analysis of the momentum equation (4) shows that the pressure term and the momentum terms may be neglected by comparison with either of the shear stress terms. Thus τ_w may still be assumed equal to τ_v , although τ_v is no longer X-independent -

$$\text{As before, } u = \frac{g_0 \tau_v y}{\mu}$$

The energy equation becomes, as before,

$$\frac{2\mu K \Delta T}{g_0 \rho \lambda^2} = \delta \frac{d}{dx} (\tau_v \delta^2) \quad (15)$$

However, τ_v is no longer constant.

Assuming $\tau_v = f \frac{\rho_v u_v^2}{2g_0}$ where f is constant

then $\tau_v = \tau_{v0} \left(\frac{u_v}{u_{v0}} \right)^2$ (16)

Where τ_{v0} , u_{v0} are the initial values of shear stress and vapor velocity.

(12)

From considerations of continuity, for condensation on one wall of the duct,

$$\rho_v u_v (a-\delta) + \int_0^{\delta} \rho_v u_v dy = \rho_v u_{v0} a \quad (17)$$

Substituting (5) in (17)

$$\rho_v u_v (a-\delta) + \frac{1}{\lambda'} \int_0^x \frac{K\Delta T}{\delta} dx = \rho_v u_{v0} a \quad (18)$$

$$\frac{u_v}{u_{v0}} = \frac{1}{(1 - \frac{\delta}{a})} \left[1 - \frac{1}{\rho_v u_{v0} a \lambda'} \int_0^x \frac{K\Delta T}{\delta} dx \right] \quad (19)$$

For condensation on both walls, the equivalent equation is

$$\frac{u_v}{u_{v0}} = \frac{1}{(1 - \frac{2\delta}{a})} \left[1 - \frac{2}{\rho_v u_{v0} a \lambda'} \int_0^x \frac{K\Delta T}{\delta} dx \right] \quad (20)$$

Equations (15), (16) and (19) may be solved for δ as a power series in X .

(13)

The solution is

$$\delta = Ax^{1/3} \left[1 + \frac{6K\Delta T x^{2/3}}{5Au_{vo}\rho_v\lambda'a} - \frac{3Ax^{1/3}}{4a} \right] \quad (21)$$

+ Higher order terms

$$\text{where } A = \left[\frac{3K\Delta T \mu x}{\rho g_o \tau_{vo} \lambda' a} \right]^{1/3}$$

The first term in the bracket is the flat plate solution, equation 11. The second term is the first-order correction for the reduction of shear stress due to vapor condensation, and the third term is the first-order correction for the blockage of the channel by the film. In most cases the third term is an order of magnitude smaller than the second term and can be neglected. In general, for up to 20% condensation, an excellent approximation is

$$\delta = Ax^{1/3} \left[1 + (n) \frac{6K\Delta T \mu x^{2/3}}{5Au_{vo}\rho_v\lambda'a} \right] \quad (22)$$

where n is 1 for condensation on one side

n is 2 " " " both sides

(14)

To the same approximation, the vapor velocity is given by

$$u_v = u_{v0} \left[1 - (n) \frac{3K\Delta T x^{2/3}}{2A\rho_v \lambda' a u_{v0}} \right] \quad (23)$$

As before, the heat transfer coefficient is calculated from the equation (12)

$$h_m \Delta T x = \frac{\rho \tau_v(x) g_0 \delta^2 \lambda'}{2\mu}$$

where

$$\tau_v(x) = \tau_{v0} \left(\frac{u_v}{u_{v0}} \right)^2$$

$$h_m \left[\frac{\Delta T x \mu}{\rho \tau_{v0} g_0 \lambda'} \right] = \left(\frac{\tau_v}{\tau_{v0}} \right) \frac{\delta^2}{2}$$

$$h_m \left[\frac{\Delta T x \mu}{\rho \tau_{v0} g_0 \lambda'} \right] = \left(\frac{u_v}{u_{v0}} \right)^2 \frac{\delta^2}{2} \quad (24)$$

Comparison of values of h with those predicted by equation (13) demonstrates that the heat transfer coefficient is about $q/2$ percent smaller than the flat plate value, where q is the percentage of the vapor condensed over the distance x . Up to 10% condensation the flat plate values may therefore be used with very little error.

2.4 Effect of a wall resistance

We now wish to consider the effect of an additional heat transfer resistance on the film growth. Suppose that heat transfer is through the film and a wall with heat transfer coefficient h_w , and that the constant temperature difference ΔT_o is imposed across the wall and the film. Then the temperature difference across the film at any point ΔT_f is given by

$$\Delta T_f = \Delta T_o \frac{\delta}{\delta + K/h_w} \quad (25)$$

With the same assumptions as before, the energy equation is

$$K \frac{\Delta T_f}{\delta} = \frac{g_o \rho \lambda'}{2\mu} \frac{d}{dx} (\tau_v \delta^2) \quad (26)$$

Substituting (25) in (26)

$$\frac{\Delta T_o}{\delta/K + 1/h_w} = \frac{g_o \rho \lambda'}{2\mu} \frac{d}{dx} (\tau_v \delta^2) \quad (27)$$

For the simplest case of flow over a flat plate with τ_v constant, equation (27) integrates to

$$\frac{\Delta T_o \mu x}{g_o \tau_v \rho \lambda'} = \frac{\delta^3}{3K} + \frac{\delta^2}{2h_w} = F(\delta) \quad (28)$$

This equation is most easily solved by graphical means. For given values of K , h_w , $F(\delta)$ can be plotted as a function of δ . The solution of the equation is given by the positive intercept of this curve with the line

$$F(\delta) = \frac{\Delta T_o \mu x}{g_o \tau_v \rho \lambda'} \quad (\text{see Figure 5}).$$

The heat transfer coefficient is found from equation (12).

$$h_m \Delta T_o x = \frac{\rho \tau_v g_o \lambda' \delta^2}{2\mu}$$

$$h_m \left(\frac{\Delta T_o \mu x}{g_o \tau_v \rho \lambda'} \right) = \frac{\delta^2}{2} \quad (29)$$

$$\text{or} \quad h_m = \frac{\delta^2}{2F(\delta)} \quad (30)$$

The heat transfer coefficient can be rapidly calculated as a function of $F(\delta)$, i.e. of $\frac{\Delta T_o \mu x}{g_o \tau_v \rho \lambda'}$.

3. EXPERIMENTS

3.1 Apparatus

To investigate the validity of the theory, some simple experiments were carried out with condensing steam in a horizontal duct. Only the bottom plate of the duct was cooled, to eliminate interference from condensate running down the side walls. A schematic of the entire apparatus is shown in Figure 6 and a more detailed drawing of the duct in Figure 7. Figures 8 and 9 are photographs of the test rig. Saturated boiler steam at about 150 psi was taken from the main steam line and throttled down to atmospheric pressure, leaving the throttle valve with 150° superheat. The superheat was then removed by water injection and the steam entered the steam chest at about 215°F. Inside the steam chest was a 5 foot long sheet metal duct of rectangular cross section 3" by 1 1/2". The steam entered the duct and passed through a four foot uncooled portion to establish an equilibrium wall shear stress before flowing through a one foot section in which the bottom plate was water cooled. The condensate was collected in a measuring cylinder from a drain slot at the end of the test section. The remaining steam

flowed on through the duct and was exhausted through an ejector.

Wall shear stress was measured by averaging the pressure drop from three static pressure taps ahead of the test section. Steam velocity was obtained from a pitot-static tube. The overall temperature difference between the cooling water and the steam was obtained from the steam temperature and the average cooling water temperature.

For a valid comparison between theory and experiment, it was essential that gravity forces on the film be negligible. This was accomplished by careful adjustment of the duct to a horizontal position, and by ensuring that the conditions of the experiment were such that the weight of the film per square foot was never much greater than the vapor shear stress. Thus, a duct inclination of several degrees from horizontal would be needed to introduce a body force effect of 10% of the shear force.

Steam velocities were from 40 ft/sec to 80 ft/sec.

Most of the test points were taken with average cooling water temperatures in the range 50° to 100° . Attempts were made to run with lower overall ΔT , but the hot water supply limited the duration of a run to only a few minutes at a ΔT of 50° , and the measurements were of very doubtful accuracy.

One major uncertainty in measurement was in wall

shear stress, for the static pressure drop per foot was only of the order of 0.01" water and steam condensation in the tubing between the test section and the inclined manometer added to the difficulty of measurement. However, even if an error of $\pm 50\%$ in shear stress is considered as possible, this still introduces an error of only $\pm 15\%$ in predicted heat transfer coefficients since the cube root of shear stress appears in equation (13).

The other major uncertainty was in measurement of the condensation rate. This was accomplished by collecting the condensate running out of the drain slot behind the test section. At a given test condition the collection rate was found to be strongly dependent on the difference in static pressure between the test section and the room. Figure 10 shows the variation in collection rate with pressure differential. When the test section pressure was greater than the room pressure, both steam and condensate flowed out of the drain slot. As the pressure differential was reduced the liquid flow rate dropped and the volume of steam leakage fell also. When the test section pressure was lowered below the room pressure, air was aspirated into the duct through the drain slot and

if the test section pressure was 0.6 " water less than the room pressure the condensate ceased to flow out at all. In all cases, care was taken to maintain zero mean pressure differential between the test section and the room. However, the possibility of up to 30cc/min condensate entrainment by the steam must be considered (20% to 30% of the measured condensation rate).

To obtain one test point the operator waited until temperatures were steady and then collected condensate for a period of about five minutes. During this period, unavoidable fluctuations in collection rate would occur due to small changes in ejector vacuum. In some cases a variation of $\pm 20\%$ about the mean value of collection rate was obtained in successive periods of time. This variation is the major cause of scatter in the data.

From the measurements, overall heat transfer coefficients were calculated by dividing the heat transfer rate by the product of the overall temperature difference and the test section area, which was taken as 0.275 square feet including a small allowance for the fin effect of the vertical side walls. A value

of 1000 BTU/lb was used for the modified latent heat λ' .

The film Reynolds number $\frac{4\Gamma}{\mu}$ never exceeded 400, so that the assumption can be made that the film was always laminar.

3.2 Results

The fraction of the vapor condensed in the test section never exceeded 10%. The experimental values of heat transfer coefficient may therefore be compared with the flat plate theory of section 2.4 with a maximum error of 5% resulting from neglect of the effect of changing vapor velocity.

In Figure 11, the measured overall heat transfer coefficients are plotted against the quantity $\frac{\Delta T_o \mu x}{g_o \tau_v \rho \lambda'}$. The liquid properties at saturation temperature (212°F) were used because the saturation temperature is more convenient for design purposes than the average film temperature, and the scatter was not appreciably reduced by employing average film temperature properties.

On the same figure, predicted values of overall heat transfer coefficient from equations (28) and (30) are plotted for values of h_m of ∞ , 1000, and 650 BTU/ft² hr °F. The measured values of overall heat transfer coefficient are from 50% to 70% of the

theoretical values for zero wall resistance. They are within $\pm 20\%$ of the line for h_w equal to $650 \text{ BTU/ft}^2\text{hr}^\circ\text{F}$, which is somewhat larger than the estimated value of h_w assuming turbulent flow on the coolant side of the test section.

From this comparison, we can certainly conclude that the actual film coefficients are at least half of the theoretical values. In addition, it seems highly probable that the wall resistance is close to $650 \text{ BTU/ft}^2\text{hr}^\circ\text{F}$, in which case the theory is valid within the usual limitations of heat transfer correlations. For conservative design purposes the film coefficient could be taken as 75% of the theoretical flat plate values in the laminar flow regime.

List of Symbols

a	Plate spacing
C	Liquid specific heat
f	Friction factor
g_0	Constant in Newton's 2nd Law.
h_m	Average overall heat transfer coefficient
h_w	Wall heat transfer coefficient
K	Thermal conductivity of liquid
p	Pressure
q	Fraction of vapor condensed
T	Temperature
ΔT	Temperature difference
u	Velocity along surface
v	Velocity perpendicular to surface
x	Distance along plate from beginning of condensation
y	Distance perpendicular to plate
Γ	Film mass flow per unit width
δ	Film thickness
ρ	Density
μ	Viscosity
ν	Kinematic viscosity
λ	Latent heat of condensation

λ Latent heat of condensation

λ' $\lambda + \frac{C\Delta T}{3}$

τ Shear stress

Subscripts

o Initial value

s Saturation

δ At $y=\delta$

w Wall

v Vapor

References

1. W. Nusselt 'Die oberflächen Kondensation des wasserdampfes' Zeitschrift des Vereines Deutcher Ingenieure Vol. 60, 1916 p. 541.
2. W. M. Rohsenow, J. H. Webber, A. T. Ling , Effect of vapor velocity on laminar and turbulent film condensation'. ASME Trans. 1956 pp. 1637-1643.
3. W. M. Rohsenow 'Heat transfer and temperature distribution in laminar-film condensation' ASME Trans. 1956 pp. 1645-1648.
4. F. M. Sparrow, J. L. Gregg 'A boundary-layer treatment of laminar-film condensation' ASME Journal of Heat Transfer February 1959. pp. 13-18.

List of Figures

1. Schematic of vapor condensation on an inclined plate under gravity force.
2. Element of condensate layer.
3. Flat plate heat transfer coefficient under zero gravity.
4. Schematic of duct.
5. Graphical solution of cubic equation.
6. Layout of experimental equipment.
7. Drawing of test section.
8. Photograph of test rig.
9. Close-up of test section.
10. Effect of pressure differential on condensate measurement.
11. Heat transfer coefficient as function of $\frac{\Delta T_o \mu x}{g_o \tau \nu \rho \lambda^3}$

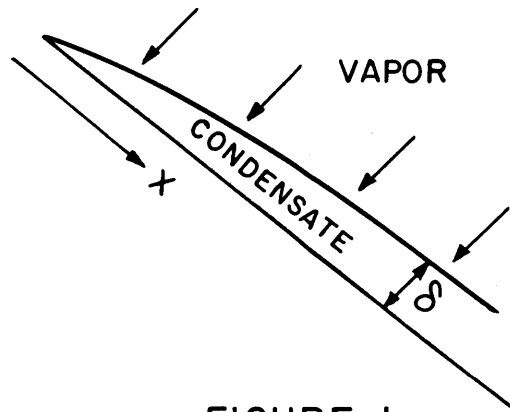


FIGURE 1

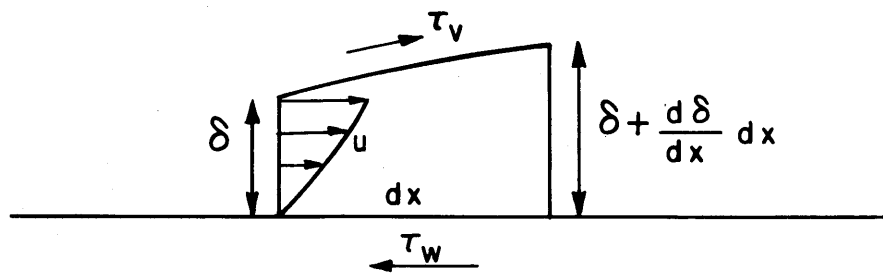


FIGURE 2

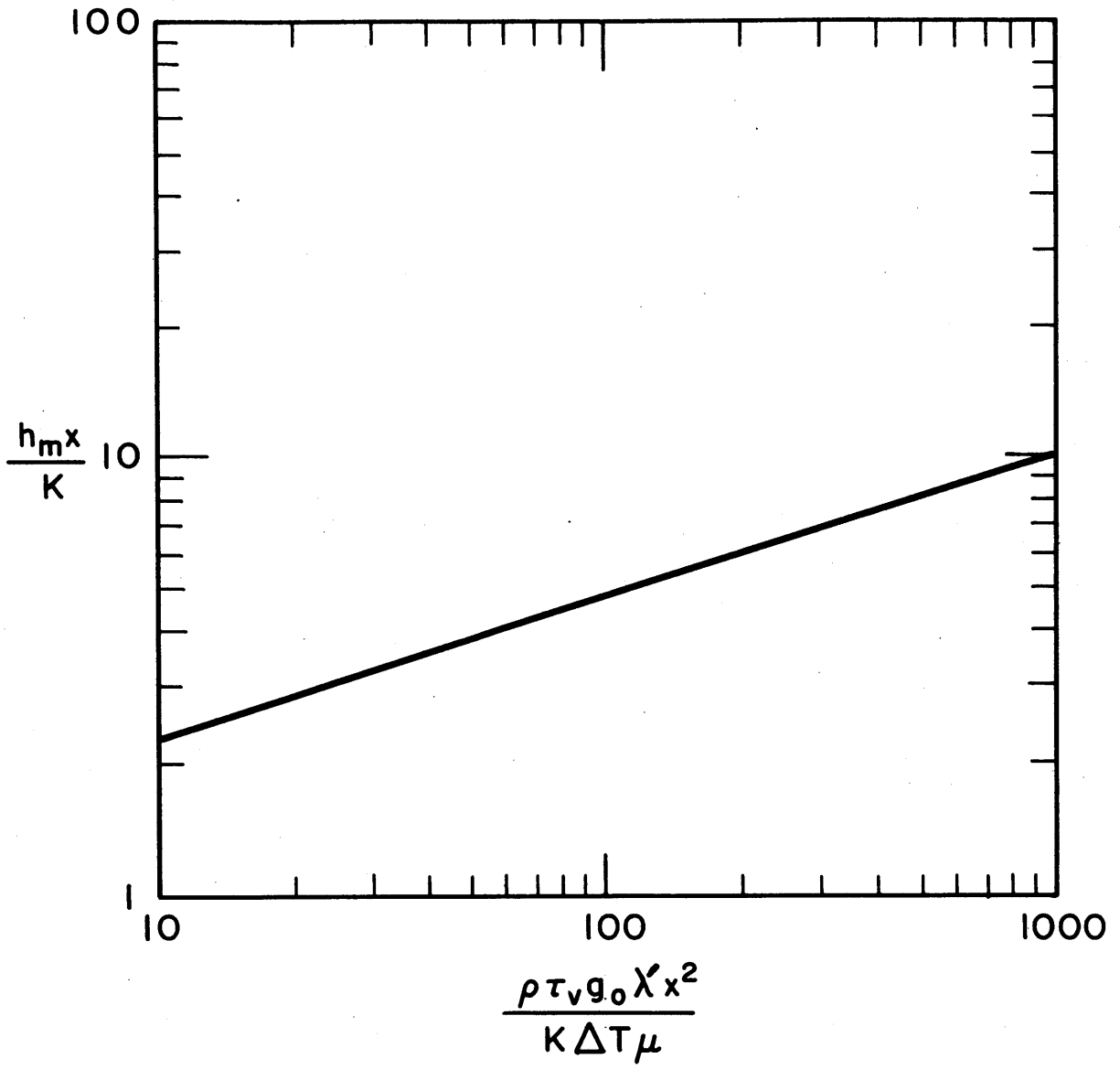


FIGURE 3

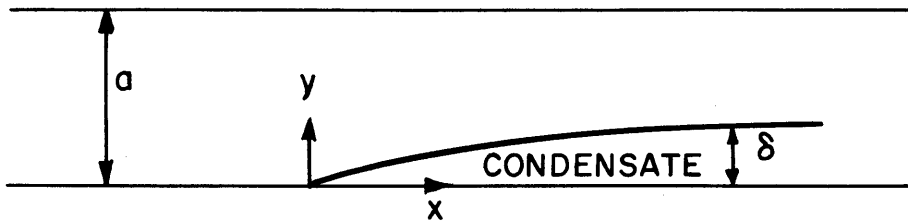


FIGURE 4

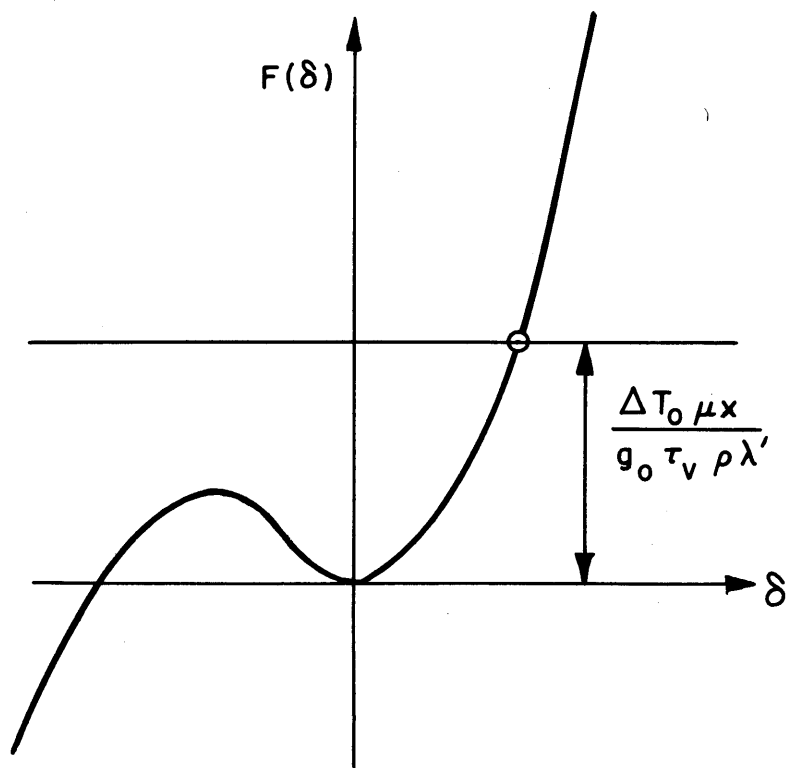


FIGURE 5

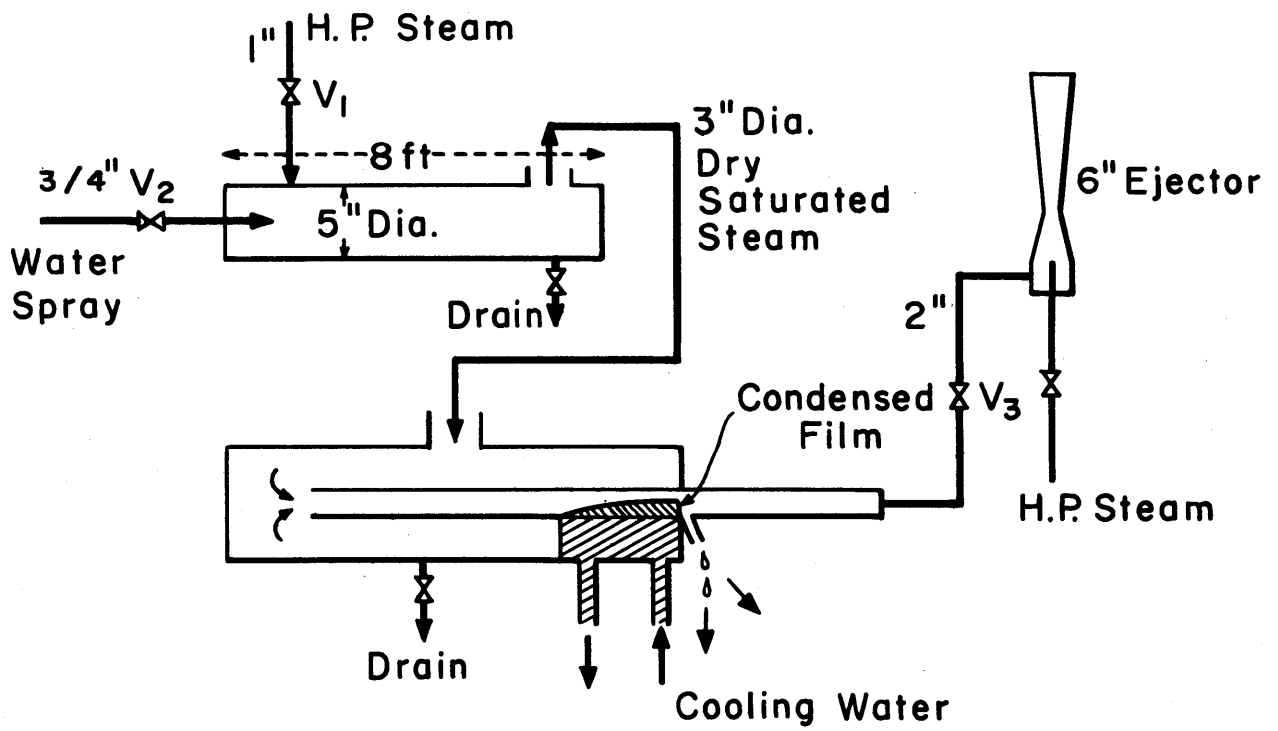


FIGURE 6

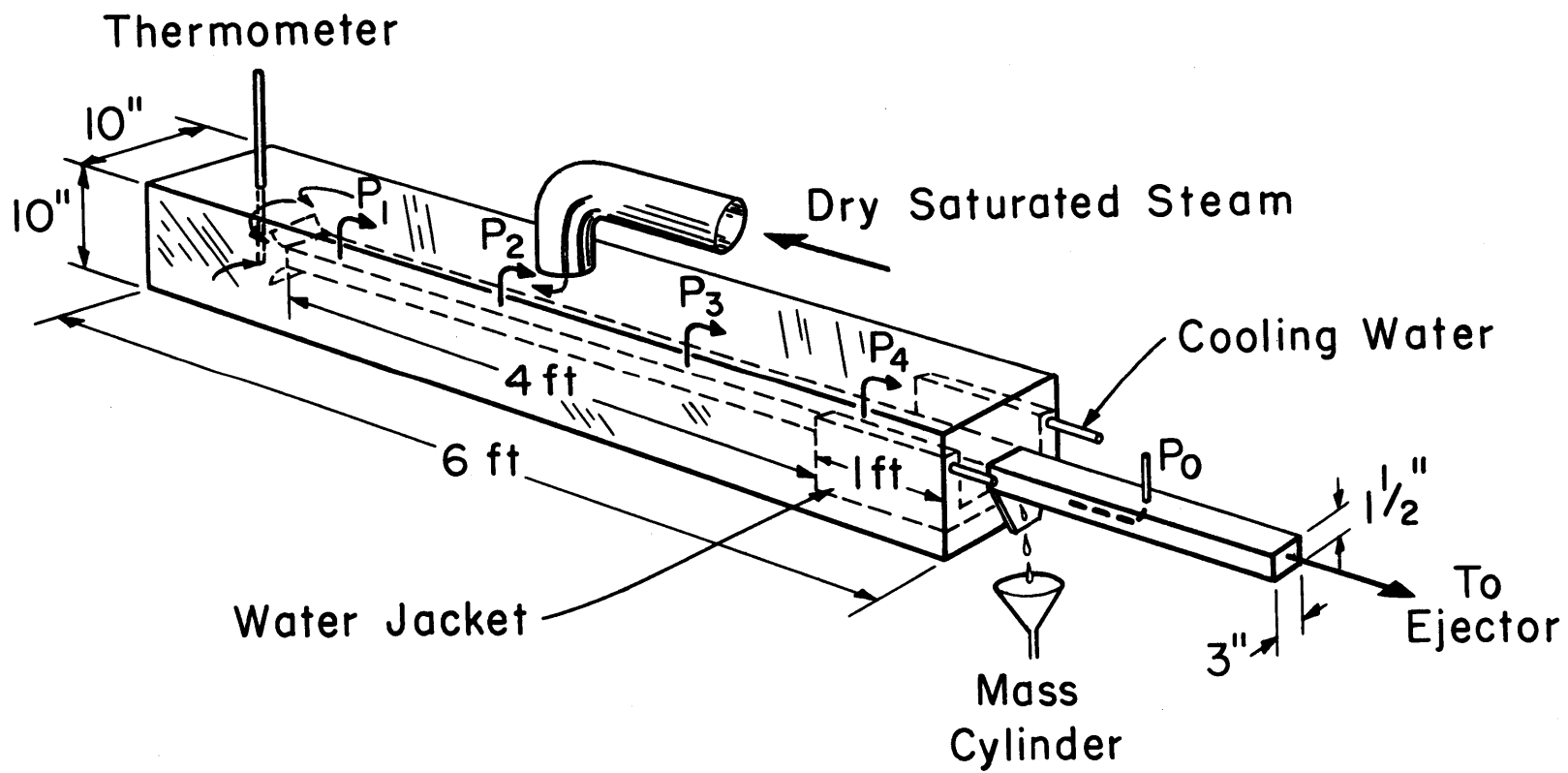


FIGURE 7

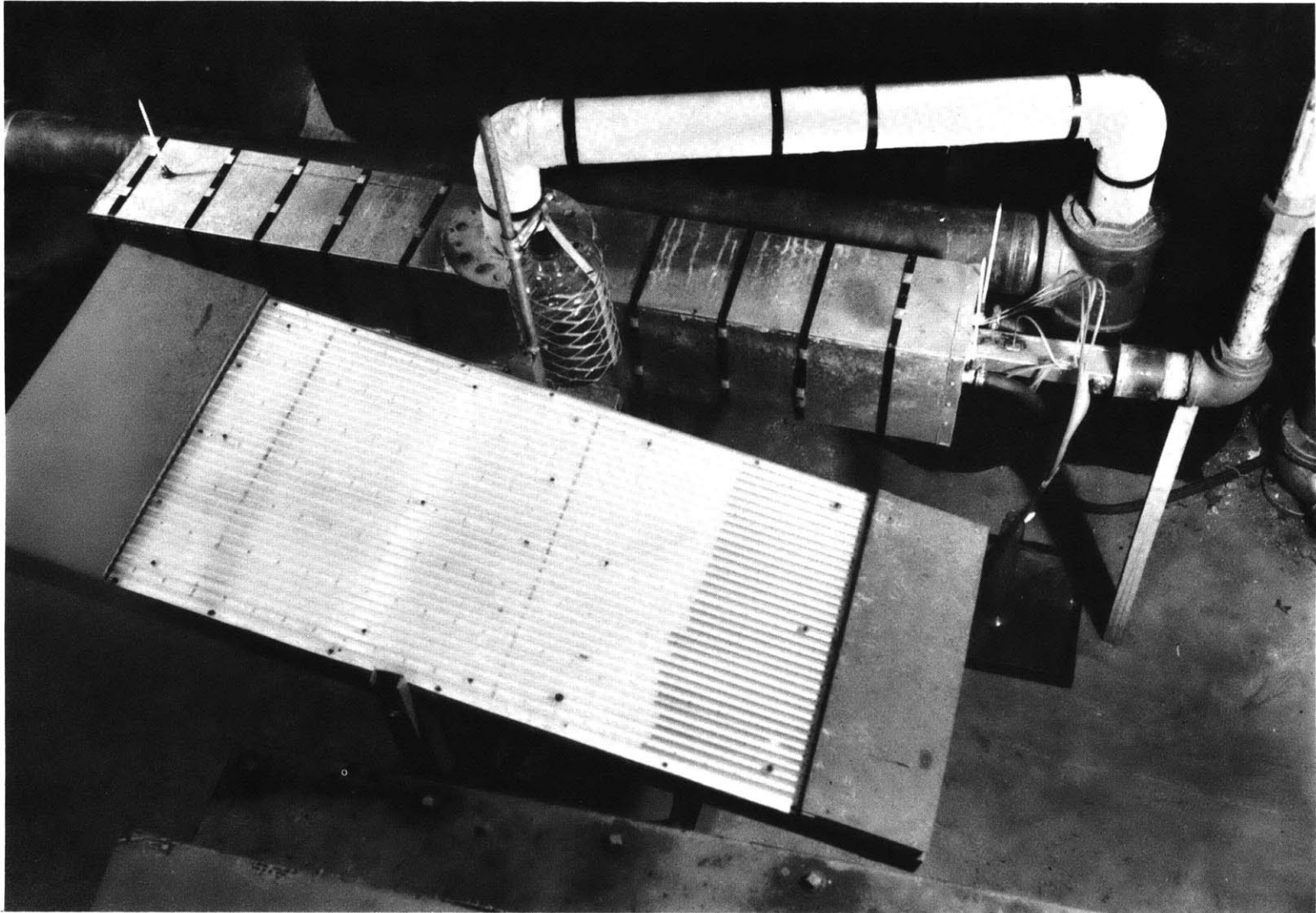


FIGURE 8

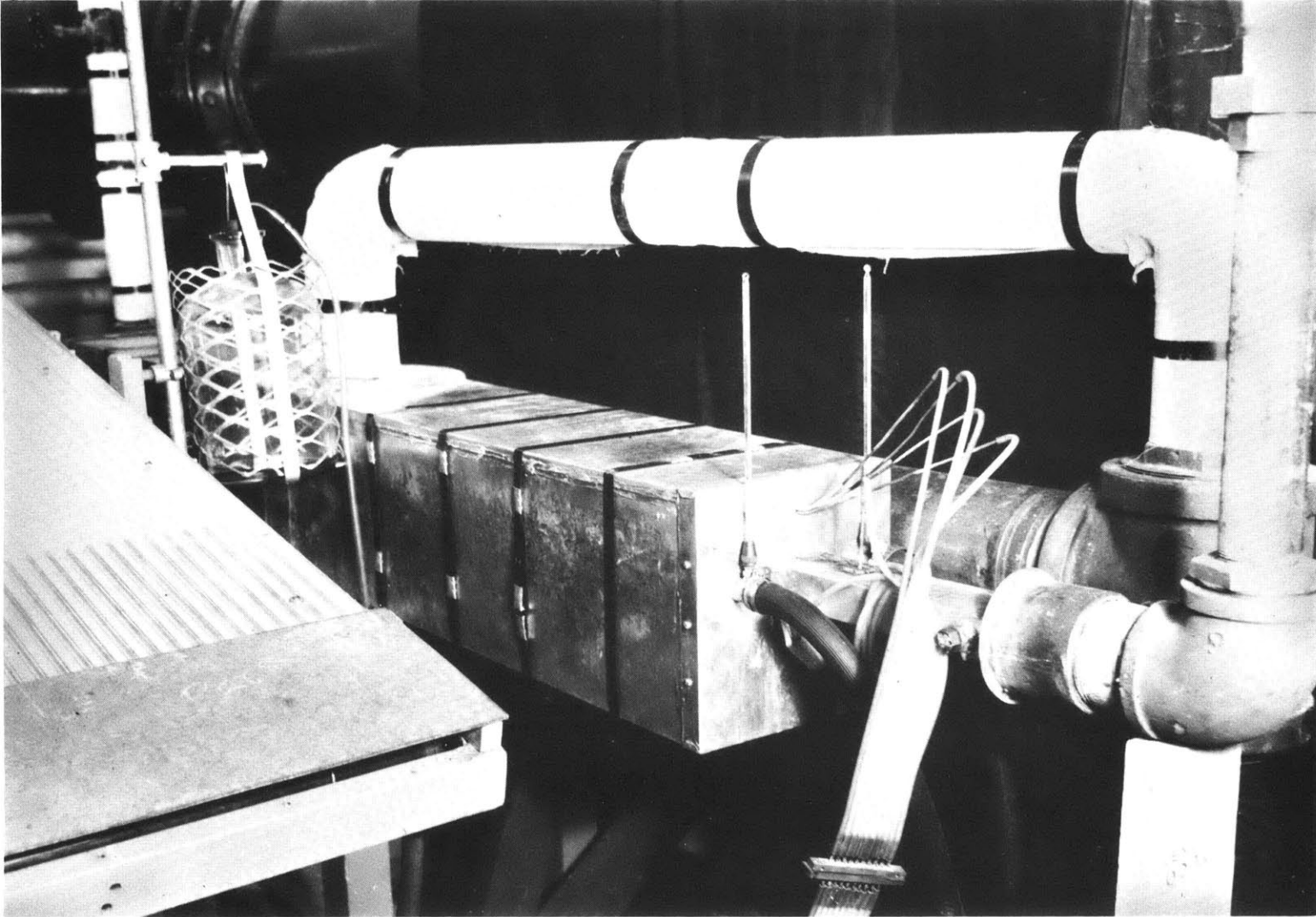


FIGURE 9

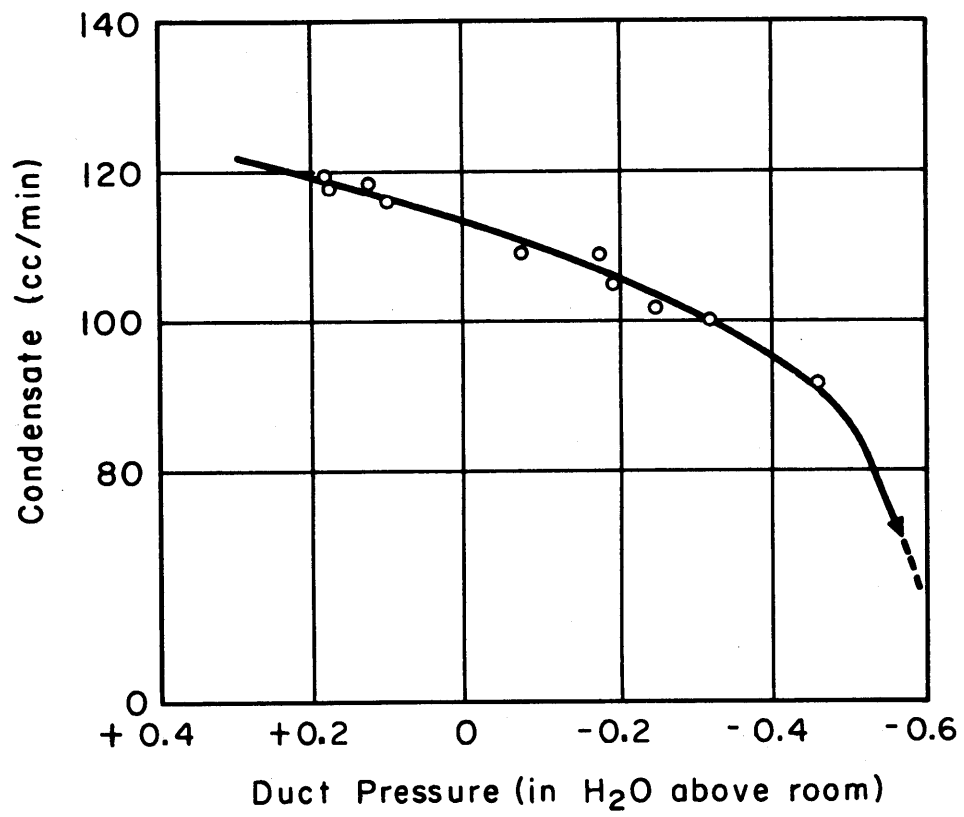


FIGURE 10

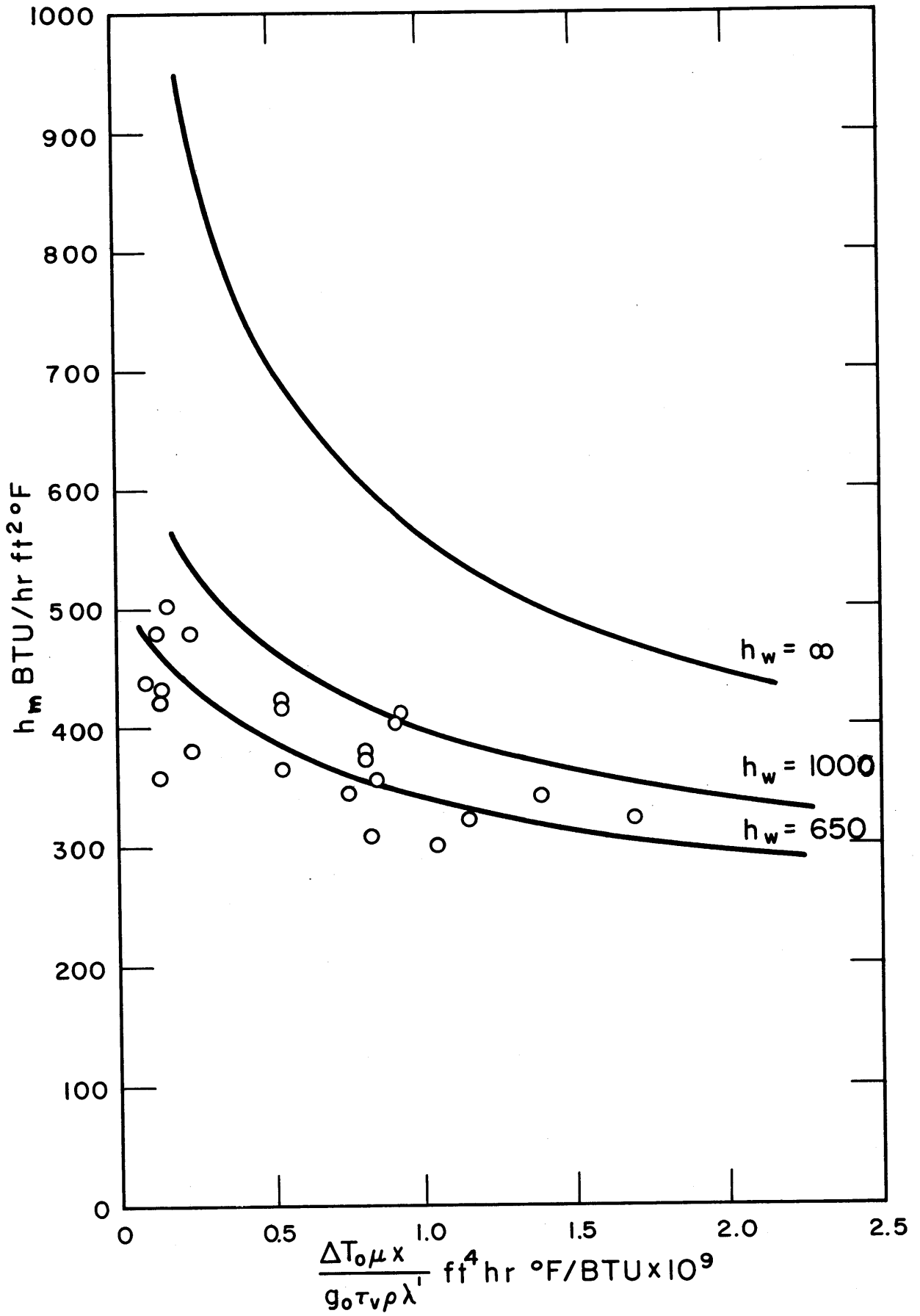


FIGURE II